Received June 1999
Revised November 1999
Accepted November 1999

Non-similar solutions for heat and mass transfer by hydro-magnetic mixed convection flow over a plate in porous media with surface suction or injection

Ali J. Chamkha
Department of Mechanical and Industrial Engineering, Kuwait University, Safat, Kuwait

Keywords *Heat transfer, Convection, Finite differences, Porous medium, Numerical solutions*

Abstract *The problem of steady, laminar, heat and mass transfer by mixed convection from a semi-infinite, isothermal, vertical and permeable plate embedded in a uniform porous medium in the presence of temperature-dependent heat source or sink and magnetic field effects is considered. A mixed convection parameter for the entire range of free-forced-mixed convection is employed and non-similar equations are obtained. These equations are solved numerically by an efficient implicit, iterative, finite-difference scheme. The obtained results are checked against previously published work on special cases of the problem and are found to be in good agreement. Useful correlations for the local Nusselt number are obtained for various physical parameters. A parametric study illustrating the influence of the magnetic field, porous medium inertia effects, heat generation or absorption, concentration to thermal buoyancy ratio, and the Lewis number on the fluid velocity, temperature and concentration as well as the Nusselt and the Sherwood numbers is conducted. The obtained results are shown graphically and the physical aspects of the problem are discussed.*

Nomenclature

B_o = Magnetic field strength
C = Dimensionless concentration at any point in the flow field
c = Concentration at any point in the flow field
c_∞ = Concentration at the free stream
c_w = Concentration at the wall
D = Mass diffusivity
F = Inertia coefficient of the porous medium
f = Dimensionless stream function $f = \psi/(\alpha_e(Pe_x^{1/2} + Ra_x^{1/2}))$
g = Gravitational acceleration
h = Local convective heat transfer coefficient
h_m = Local mass transfer coefficient
K = Permeability of the porous medium
ke = Porous medium effective thermal conductivity
L = Characteristic length
Le = Lewis number ($Le = \alpha_e/D$)
M = Square of the Hartmann number ($M = (\sigma B_o K)/(\varepsilon\mu)$)
N = Buoyancy ratio ($N=(\beta_c(c_w - c_\infty))/(\beta_T(T_w - T_\infty))$)
Nu_x = Local Nusselt number ($Nu_x=hx/k_e$)
p = Fluid pressure
Pe_x = Local Peclet number ($Pe_x=V_\infty x\alpha_e$)
Pe_L = Peclet number at x=L
Qo = Heat generation or absorption coefficient
Ra_x = Local Rayleigh number ($Ra_x=\rho g\beta_T K|T_w - T_\infty((x/(\mu\alpha_e))$)
Ra_L = Rayleigh number at x=L
Sh_x = Local Sherwood number ($Sh_x=h_m x/D$)
T = Temperature at any point
T_w = Wall temperature
T_∞ = Free stream temperature
u = Tangential or x-component of velocity
v = Normal or y-component of velocity

International Journal of Numerical Methods for Heat & Fluid Flow, Vol. 10 No. 2, 2000, pp. 142-162.

v_o = Wall mass transfer coefficient
V_∞ = Free stream velocity
x = Distance along the plate
y = Distance normal to the plate

Greek symbols
ε = Porosity of porous medium
Γ = Dimensionless porous medium inertia coefficient ($\Gamma = 2FK(Pe_L^{1/2} + Ra_L^{1/2})/(\mu L)$)
α_e = Effective thermal diffusivity of the porous medium
β_c = Concentration expansion coefficient
β_T = Thermal expansion coefficient
ϕ = Dimensionless heat absorption parameter ($\phi = Q_o/(\rho c_p v_o)$)
η = Coordinate transformation in terms of x and y ($\eta = y(Pe_x^{1/2} + Ra_x^{1/2})/x$)
χ = Mixed convection parameter ($\chi = (1 + (Ra_x/Pex)^{1/2})^{-1}$)
ψ = Stream function
θ = Dimensionless temperature ($\theta = (T - T_\infty)/(T_w - T_\infty)$)
ρ = Fluid density
σ = Fluid electrical conductivity
ξ = Transformed suction or injection parameter ($\xi = v_o x(Pe_x^{1/2} + Ra_x^{1/2})^{-1}/\alpha_e$)

Introduction

Recently, there has been increased interest in investigating buoyancy-induced flow by simultaneous heat and mass transfer from different geometries embedded in porous media. This interest stems from the fact that these flows have many engineering and geophysical applications such as geothermal reservoirs, drying of porous solids, thermal insulation, enhanced oil recovery, packed bed catalytic reactors, cooling of nuclear reactors, and underground energy transport. Most early studies on porous media have used the Darcy law, which is a linear empirical relation between the Darcian velocity and the pressure drop across the porous medium and is limited to slow flows. However, for high velocity flow situations, the Darcy law is inadequate for predicting the proper physical flow behavior since it neglects the porous medium inertia effects, which become important. In this situation, the pressure drop across the porous medium is a quadratic function of the flow rate. It has been reported that the high flow situation is established when the Reynolds number based on the pore size is greater than unity. Vafai and Tien (1981) have discussed the importance of inertia effects for flows in porous media.

Cheng and Minkowycz (1977) have presented similarity solutions for free thermal convection from a vertical plate in a fluid-saturated porous medium. The problem of combined thermal convection from a semi-infinite vertical plate in the presence or absence of a porous medium has been studied by many authors (see, for example, Minkowycz *et al.*, 1985a; Ranganathan and Viskanta, 1984; Nakayama and Koyama, 1987; Hsieh *et al.,* 1993). Nakayama and Koyama (1987) have suggested similarity transformations for pure, combined and forced convection in Darcian and non-Darcian porous media. Lai (1991) has investigated coupled heat and mass transfer by mixed convection from an isothermal vertical plate in a porous medium. Hsieh *et al.* (1993) have presented non-similar solutions for combined convection in porous media.

There has been a renewed interest in studying magnetohydrodynamic (MHD) flow and heat transfer in porous and non-porous media due to the effect of magnetic fields on flow control and on the performance of many systems using electrically-conducting fluids. For example, Raptis *et al.* (1982a) have

analyzed hydromagnetic free convection flow through a porous medium between two parallel plates. Aldoss *et al.* (1995) have studied mixed convection from a vertical plate embedded in a porous medium in the presence of a magnetic field. Bian *et al.* (1996) have reported on the effect of an electromagnetic field on natural convection in an inclined porous medium. Buoyancy-driven convection in a rectangular enclosure with a transverse magnetic field has been considered by Garandet *et al.* (1992) and Khanafer and Chamkha (1998).

In certain porous media applications such as those involving heat removal from nuclear fuel debris, underground disposal of radioactive waste material, storage of food stuffs, and exothermic chemical reactions and dissociating fluids in packed-bed reactors, the working fluid heat generation (source) or absorption (sink) effects are important. Analysis of these situations requires the addition of a heat source or sink term in the energy equation. This term has been assumed to be either a constant (Acharya and Goldstein, 1985; Song, 1996), space-dependent and/or temperature-dependent (Vajravelu and Nayfeh, 1992; Chamkha, 1996; 1997).

The effects of fluid wall suction or injection the flow and heat transfer characteristics along vertical semi-infinite plates have been investigated by several authors (Cheng, 1977; Lai and Kulacki, 1990a,b; Minkowycz *et al.,* 1985b; Hooper *et al.*, 1993). Some of these studies have reported similarity solutions (Cheng, 1977; Lai and Kulacki, 1990a,b), while others have obtained non-similar solutions, (Minkowycz *et al.*, 1985b; Hooper *et al.,* 1993). For example, Lai and Kulacki (1990a,b) have reported similarity solutions for mixed convection flow over horizontal and inclined plates embedded in fluid-saturated porous media in the presence of surface mass flux. On the other hand, Minkowycz *et al.* (1985b) have discussed the effect of surface mass transfer on buoyancy-induced Darcian flow adjacent to a horizontal surface using non-similarity solutions. More recently, Hooper *et al.* (1993) have considered the problem of non-similar mixed convection flow along an isothermal vertical plate in porous media with uniform surface suction or injection and introduced a single parameter for the entire regime of free-forced-mixed convection. Their non-similar variable represented the effect of suction or injection at the wall.

The objective of this paper is to generalize the work of Hooper *et al.* (1993) and consider simultaneous heat and mass transfer by mixed convection from a permeable vertical plate embedded in a fluid-saturated porous medium in the presence of suction or insection, magnetic field effects, heat generation or absorption effects, and porous medium inertia effects. This will be done for isothermal and isoconcentration wall conditions in the entire range of free-forced-mixed convection regime.

Problem formulation

Consider steady hydromagnetic mixed convection from a permeable semi-infinite vertical plate embedded in a porous medium in the presence of heat generation (source) or absorption (sink). Uniform suction or injection with

speed v_o is imposed at the plate surface. A uniform magnetic field is applied in the horizontal direction normal to the plate. The porous medium is assumed to be uniform, isotropic and in thermal equilibrium with the plate. Let the plate be maintained at a constant temperature T_w and concentration c_w and the free stream velocity, temperature and concentration be V_∞, T_∞ and C_∞, respectively. Further assume that all fluid properties are constant except the density in the body force term of the linear momentum balance. Under the Boussinesq and boundary-layer approximations, the governing equations for this problem can be written as

$$\frac{\partial u}{\partial x} + \frac{\partial v}{\partial y} = 0 \tag{1}$$

$$\left(1 + \frac{\sigma B_o^2 K}{\varepsilon \mu} + \frac{2FK}{\mu} u\right) \frac{\partial u}{\partial y} = \frac{K}{\mu} \rho g \left(\beta_T \frac{\partial T}{\partial y} + \beta_c \frac{\partial c}{\partial y}\right) \tag{2}$$

$$u \frac{\partial T}{\partial x} + v \frac{\partial T}{\partial y} = \alpha_e \frac{\partial^2 T}{\partial y^2} + \frac{Q_o}{\rho c_p} (T - T_\infty) \tag{3}$$

$$u \frac{\partial c}{\partial x} + v \frac{\partial c}{\partial y} = D \frac{\partial^2 c}{\partial y^2} \tag{4}$$

where x and y denote the vertical and horizontal directions respectively. u, v, T and c are the x- and y-components of velocity, temperature and concentration respectively. ρ, μ, σ, c_p and D are the fluid density, dynamic viscosity, electrical conductivity, specific heat at constant pressure, and mass diffusion coefficient respectively. K, ε, F, and α_e are the porous medium permeability, porosity, Forcheimer constant, and effective thermal diffusivity, respectively. B_o, β_T, β_c and Q_o are the magnetic induction, thermal expansion coefficient, concentration expansion coefficient, and heat generation (>0) or absorption (<0) coefficient respectively.

It should be noted that equation (2) is obtained by using the modified Brinkman extension of Darcy law which includes the porous medium inertia effects, magnetic effects and thermal and concentration buoyancy effects and neglects the convective terms and then differentiating with respect to y in order to eliminate the pressure gradient term by using the y-momentum equation (after differentiating with respect to x) which gives $\frac{\partial^2 p}{\partial x \partial y} = 0$.

The boundary conditions suggested by the physics of the problem are

$$\begin{aligned} &v(x,0) = v_o \ , \ T(x,0) = T_w \ , \ c(x,0) = c_w \\ &u(x,\infty) = V_\infty \ , \ T(x,\infty) = T_\infty \ , \ c(x,\infty) = c_\infty \end{aligned} \tag{5}$$

It is convenient to transform the governing equations into a non-similar dimensionless form which can be suitable for solution as an initial-value

problem. This can be done by introducing the stream function such that

$$u = \frac{\partial \psi}{\partial y} \ , \ v = -\frac{\partial \psi}{\partial x} \tag{6}$$

and using

$$\eta = \frac{y}{x}\left(Pe_x^{1/2} + Ra_x^{1/2}\right) \ , \ \xi = \frac{v_o x}{\alpha_e}\left(Pe_x^{1/2} + Ra_x^{1/2}\right)^{-1} \tag{7}$$

$$\psi = \alpha_e\left(Pe_x^{1/2} + Ra_x^{1/2}\right) f(\xi,\eta) \ , \ \theta(\xi,\eta) = \frac{T - T_\infty}{T_w - T_\infty} \ , \ C(\xi,\eta) = \frac{c - c_\infty}{c_w - c_\infty} \tag{8}$$

where $Pe_x = V_\infty x/\alpha_e$ and $Ra_x = g\beta_T|T_w - T_\infty|Kx/(\nu\alpha_e)$ are the local Peclet and Rayleigh numbers respectively.

Substituting equations (6) through (8) into equations (1) through (5) produces

$$(1 + M + \Gamma f)f'' \ = \ (1 - \chi)^2(\theta + N\,C') \tag{9}$$

$$\theta'' + \frac{1}{2}f\theta' + \xi^2\phi\theta = \frac{1}{2}\xi(f'\frac{\partial\theta}{\partial\xi} - \theta'\frac{\partial f}{\partial\xi}) \tag{10}$$

$$Le^{-1}C'' + \frac{1}{2}fC = \frac{1}{2}\xi(f'\frac{\partial C}{\partial\xi} - C'\frac{\partial f}{\partial\xi}) \tag{11}$$

$$\begin{aligned} &f(\xi,0) + \xi\frac{\partial f}{\partial\xi}(\xi,0) = -2\xi \ \text{ or } f(\xi,0) = -\xi \ , \ \theta(\xi,0) = 1 \ , \ C(\xi,0) = 1 \\ &f(\xi,\infty) = \chi^2 \ , \ \theta(\xi,\infty) = 0 \ , \ C(\xi,\infty) = 0 \end{aligned} \tag{12}$$

where

$$\begin{aligned} &M = \frac{\sigma B_o^2 K}{\varepsilon\mu} \ , \ \Gamma = \frac{2FK}{\mu L}(Pe_L^{1/2} + Ra_L^{1/2}) \ , \ Le = \frac{\alpha_e}{D} \\ &N = \frac{\beta_c(c_w - c_\infty)}{\beta_T(T_w - T_\infty)} \ , \ \phi = \frac{Q_o}{\rho c_p v_o} \ , \ \chi = \left[1 + (Ra_x/Pe_x)^{1/2}\right]^{-1} \end{aligned} \tag{13}$$

are square of the Hartmann number, dimensionless porous medium inertia coefficient, Lewis number, concentration to thermal buoyancy ratio, dimensionless heat generation (>0) or absorption (<0) coefficient, and the mixed convection parameter, respectively. It should be noted that in equation (13) L is a characteristic length and that $\chi = 0(Pe_x = 0)$ corresponds to pure free convection while $\chi = 1(Ra_x = 0)$ corresponds to pure forced convection. The entire regime of mixed convection corresponds to values of χ between 0 and 1.

Of special significance for this flow and heat transfer situation are the local skin-friction coefficient and local Nusselt number. These physical quantities can be defined as

$$C_f = \frac{\tau_w}{\mu\alpha_e/x^2} = (Pe_x^{1/2} + Ra_x^{1/2})^3 f''(\xi, 0) \;\; ; \;\; \tau_w = \mu\left(\frac{\partial u}{\partial y}\right)_{y=0} \tag{14}$$

$$Nu_x = \frac{hx}{k_e} = -(Pe_x^{1/2} + Ra_x^{1/2})\theta'(\xi, 0) \; ; \; h = \frac{q_w}{T_w - T_\infty}; \;\; q_w = -k_e\left(\frac{\partial T}{\partial y}\right)_{y=0} \tag{15}$$

$$Sh_x = \frac{h_m x}{D} = -(Pe_x^{1/2} + Ra_x^{1/2})\, C'(\xi, 0)\, ; h_m = \frac{m_w}{c_w - c_\infty}; \; m_w = -D\left(\frac{\partial c}{\partial y}\right)_{y=0} \tag{16}$$

where k_e is the porous medium effective thermal conductivity and τ_w and q_w are respectively the wall shear stress and wall heat transfer.

Numerical method and validation

Equations (9) through (12) represent an initial-value problem with ξ playing the role of time. This nonlinear problem can not be solved in closed form and, therefore, a numerical solution is necessary to describe the physics of the problem. The implicit, tri-diagonal finite-difference method similar to that discussed by Blottner (1970) has proven to be appropriate and sufficiently accurate for the solution of similar problems. Therefore, it is adopted in the present investigation.

All first-order derivatives with respect to ξ are first replaced by two-point backward-difference formulae when marching in the positive ξ direction and by two-point forward-difference formulae when marching in the negative ξ direction. Then, all second-order differential equations in η are discretized using three-point central difference quotients. This discretization process produces a tri-diagonal set of algebraic equations at each line of constant ξ which is readily solved by the well known Thomas algorithm (see Blottner, 1970). During the solution, iteration is employed to deal with the non-linear nature of the governing differential equations. The problem is solved line by line starting with line $\xi = 0$ where similarity equations are solved to obtain the initial profiles of velocity, temperature and concentration and marching forward (or backward) in ξ until the desired line of constant ξ is reached. Variable step sizes in the η direction with $\Delta\eta_1 = 0.001$ and a growth factor G = 1.03 such that $\Delta\eta_n = G\Delta\eta_{n-1}$ and constant step sizes in the ξ direction with $\Delta\xi = 0.01$ are employed. These step sizes are arrived at after many numerical experimentations performed to assess grid independence. The convergence criterion employed in the present work is based on the difference between the

current and the previous iterations. When this difference reached 10^{-6} for all points in the η directions, the solution was assumed converged and the iteration process was terminated.

Tables I and II present a comparison of $-\theta'(\xi, 0)$ at selected values of ξ and χ between the results of the present work and those reported earlier by Hooper *et al.* (1993). It is clear from this comparison that a good agreement between the results exists. This lends confidence in the correctness of the numerical results to be reported subsequently. It should be noted that in Table II, the value of $-\theta'(\xi, 0)$ at $\xi = -2$ and $\chi = 1$ seems to be in error as this value cannot be 1.0502. While comparisons with experimental data would be most favorable, no such data for mixed convection appear to exist at present. However, Cheng *et al.* (1981) reported an experimental study of non-Darcian effects in free convection $\chi(= 0)$ along an impermeable ($\xi = 0$) vertical plate in a saturated porous medium. For this special case a good agreement is found between the present results and their experimental data.

Results and discussion

Figures 1 and 2 illustrate the effects of the magnetic parameter (square of Hartmann number) M on the velocity and temperature (or concentration) f', θ (or C) profiles at the end of the computational domain respectively. Application of a uniform magnetic field normal to the flow direction produces a force which acts in the negative direction of flow. This force is called the Lorentz force, which tends to slow down the movement of the electrically-conducting fluid in the vertical direction. This retardation effect is accompanied by an appreciable increase in the fluid temperature and concentration. These behaviors are clearly depicted in Figures 1 and 2. It should noted that in these figures the value of Le is taken to be unity while the value of ϕ is taken to be zero. This is done intentionally so that the effect on the temperature will be the same as that on the concentration since both become governed by the same differential equation interms of θ or C in order to minimize the number of figures.

Figures 3 and 4 show the effects of the mixed convection parameter χ on the velocity and temperature (or concentration) profiles at $\xi = 1$ respectively. From the definition of χ, it is seen that increases in the value of the parameter Ra_x/Pe_x causes the mixed convection parameter χ to decrease. Thus, small values of Ra_x/Pe_x correspond to values of χ close to unity, which indicate almost pure forced convection regime. On the other hand, high values of Ra_x/Pe_x correspond to values of χ close to zero, which indicate almost pure free convection regime. Furthermore, moderate values of Ra_x/Pe_x represent values of χ between 0 and 1, which correspond to the mixed convection regime. For the forced convection limit ($\chi = 1$) it is clear from equation (9) that the velocity in the boundary layer f′ is uniform. This is so because of the absence of the viscous term (Brinkman) from the momentum equation. However, for smaller values of χ (higher values of Ra_x/Pe_x) the buoyancy effect increases and the free stream velocity decreases. As this occurs, the fluid velocity close to the wall increases for values of $\chi \leq 0.5$ due to the buoyancy effect which becomes maximum for $\chi = 0$ (free convection limit).

Table I.
Values of $-\theta'(\xi,0)$ at selected values of ξ and χ (present work)

	$\xi=-2.0$	$\xi=-1.5$	$\xi=-1.0$	$\xi=-0.5$	$\xi=0$	$\xi=0.5$	$\xi=1.0$	$\xi=1.5$	$\xi=2.0$
$\chi=0.0$	1.99894	1.51347	1.07262	0.71213	0.44401	0.26006	0.14240	0.07248	0.03408
$\chi=0.1$	1.99793	1.50595	1.05094	0.67701	0.40375	0.22301	0.11337	0.05264	0.02214
$\chi=0.2$	1.99762	1.50265	1.03825	0.65264	0.37339	0.19439	0.09140	0.03843	0.01431
$\chi=0.3$	1.99752	1.50196	1.03398	0.64064	0.35517	0.17568	0.07686	0.02940	0.00972
$\chi=0.4$	1.99757	1.56354	1.03732	0.64149	0.35071	0.16812	0.06997	0.02496	0.00754
$\chi=0.5$	1.99824	1.50501	1.04780	0.65451	0.36045	0.17253	0.07097	0.02477	0.00725
$\chi=0.6$	2.00066	1.51648	1.06526	0.67828	0.38338	0.18901	0.08029	0.02403	0.00884
$\chi=0.7$	2.00589	1.52982	1.08954	0.71116	0.41750	0.21666	0.09824	0.03849	0.01292
$\chi=0.8$	2.01485	1.54852	1.12021	0.75148	0.46044	0.25385	0.12471	0.05408	0.02055
$\chi=0.9$	2.02831	1.57278	1.15675	0.79778	0.50998	0.29864	0.15899	0.07636	0.03289
$\chi=1.0$	2.04971	1.60251	1.19899	0.84882	0.56433	0.34826	0.19979	0.10491	0.05036

Table II.
Values of $-\theta'(\xi,0)$ at selected values of ξ and χ (Hooper *et al.*, 1993)

χ	$\xi = -2.0$	$\xi = -1.5$	$\xi = -1.0$	$\xi = -0.5$	$\xi = 0$	$\xi = 0.5$	$\xi = 1.0$	$\xi = 1.5$	$\xi = 2.0$
0.0	2.0015	1.5148	1.0725	0.7114	0.4437	0.2593	0.1417	0.0717	0.0335
0.1	2.0005	1.5076	1.0510	0.6763	0.4035	0.2223	0.1127	0.0519	0.0216
0.2	2.0003	1.5046	1.0386	0.6520	0.3732	0.1937	0.0907	0.0378	0.0139
0.3	2.0003	1.5042	1.0347	0.6401	0.3550	0.1750	0.0762	0.0288	0.0084
0.4	2.0005	1.5060	1.0384	0.6411	0.3504	0.1674	0.0693	0.0244	0.0072
0.5	2.0016	1.5106	1.0491	0.6543	0.3603	0.1719	0.0704	0.0242	0.0069
0.6	2.0042	1.5192	1.0666	0.6782	0.3832	0.1884	0.0797	0.0284	0.0085
0.7	2.0095	1.5324	1.0908	0.7111	0.4196	0.2036	0.0999	0.0339	0.0134
0.8	2.0185	1.5510	1.1214	0.7515	0.4602	0.2534	0.1242	0.0535	0.0201
0.9	2.0319	1.5751	1.1579	0.7978	0.5097	0.2982	0.1586	0.0758	0.0324
1.0	1.0502	1.6047	1.1995	0.8488	0.5642	0.3488	0.1996	0.1047	0.0502

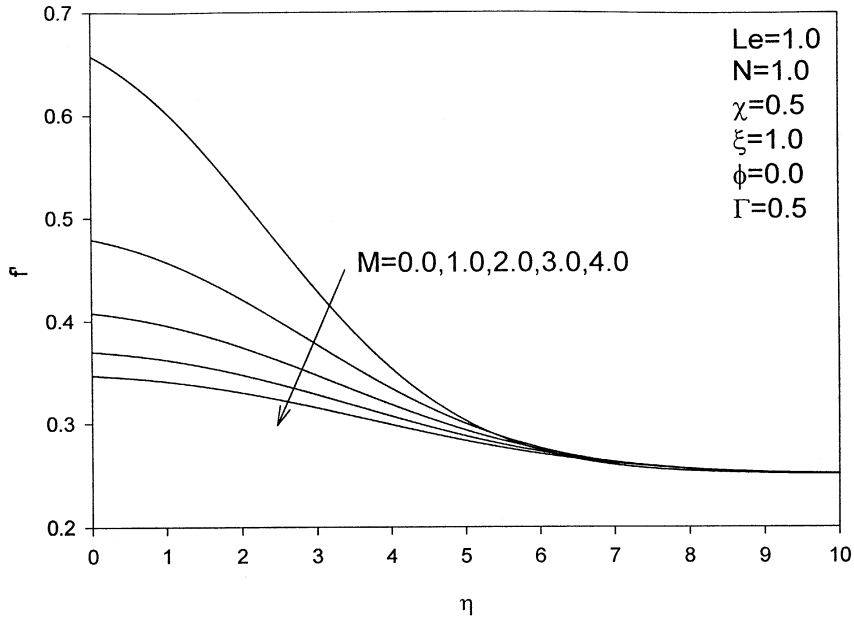

Figure 1.
Effects of M on velocity profiles

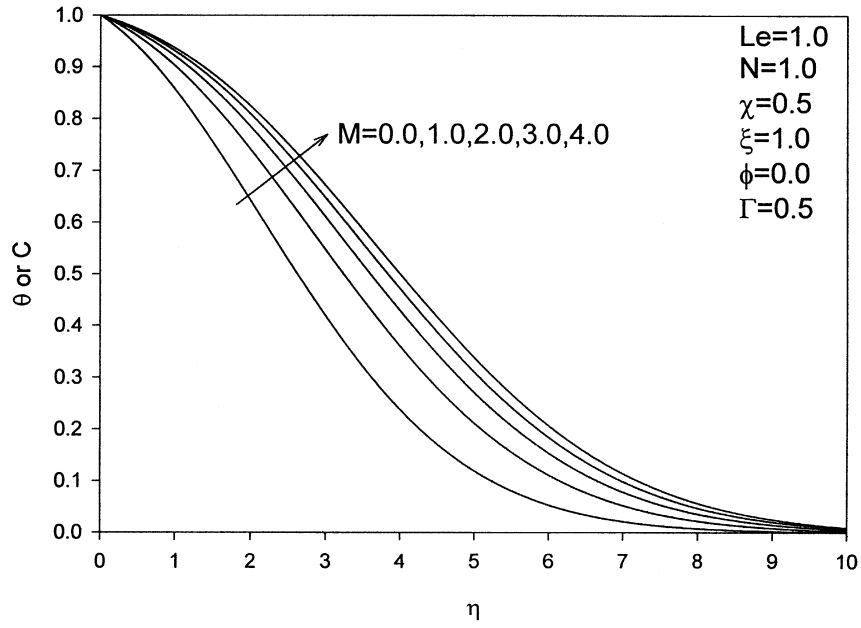

Figure 2.
Effects of M on temperature or concentration profiles

This decrease and increase in the fluid velocity f′ as χ is decreased from unity to zero is accompanied by a respective increase and a decrease in the fluid temperature or concentration. These velocity and temperature or concentration behaviors are evident from Figures 3 and 4.

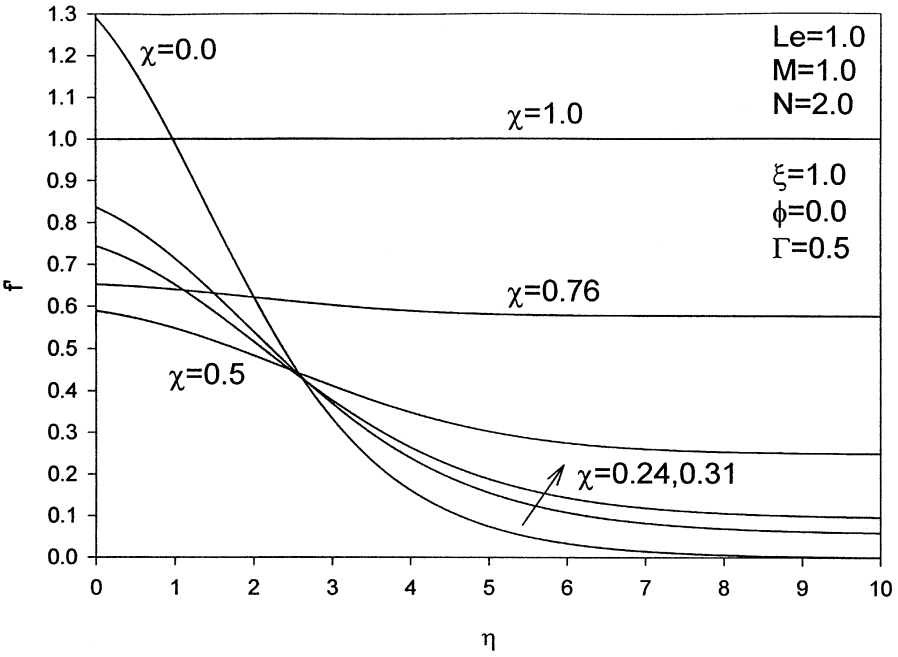

Figure 3.
Effects of χ on velocity profiles

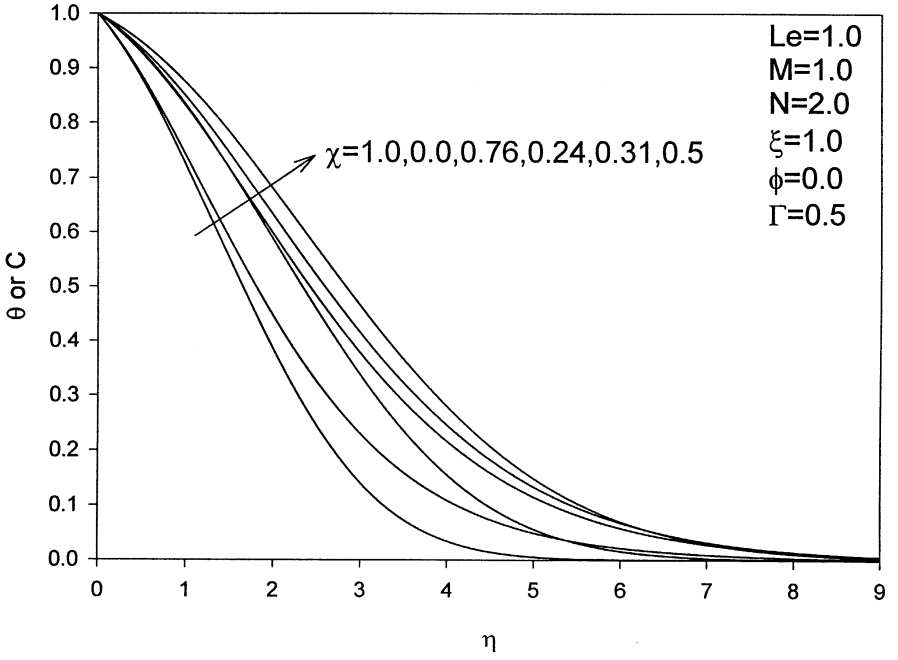

Figure 4.
Effects of χ on temperature or concentration profiles

Figures 5 and 6 present the changes in the velocity and temperature (or concentration) profiles at $\xi = 1$ that are brought about by changes in the buoyancy ratio N respectively. For a fixed value of $\chi = 0.5$ ($Ra_x/Pe_x = 1$)

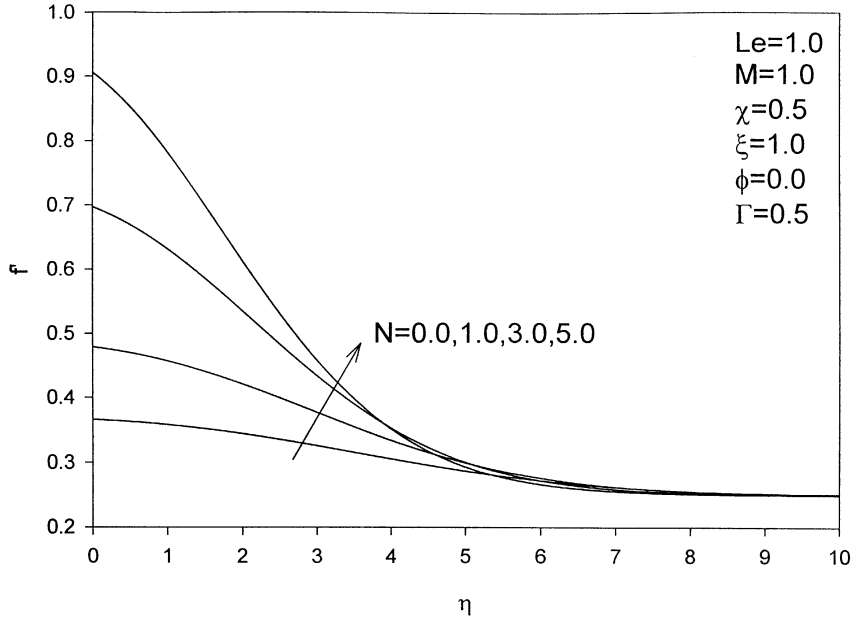

Figure 5.
Effects on N on velocity profiles

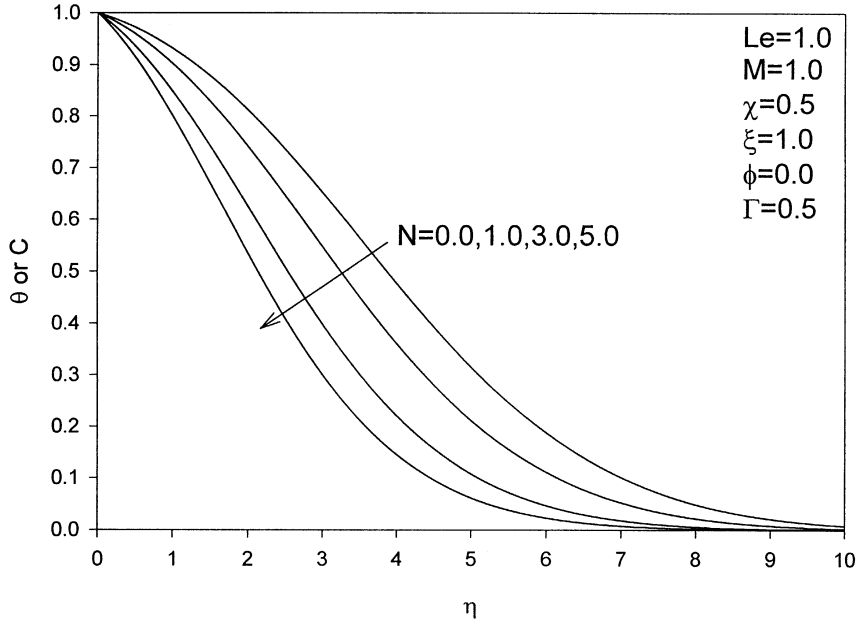

Figure 6.
Effects on N on temperature or concentration profiles

increases in the value of N have the tendency to increase the buoyancy effect, causing more induced flow along the plate in the vertical direction. This enhancement in the flow velocity is achieved at the expense of reduced fluid temperature and concentration as well as reduced thermal and concentration boundary layers as seen from Figures 5 and 6.

The effects of the heat generation or absorption coefficient ϕ on the velocity and temperature profiles at $\xi = 1$ are displayed in Figures 7 and 8 respectively. The presence of a heat generation source in the flow represented by positive values of ϕ enhances the thermal state of the fluid, causing its temperature to increase. This, in turn, increases the thermal buoyancy effect which produces higher induced flow. On the contrary, the presence of a heat absorption sink in the flow represented by negative values of ϕ reduces the fluid temperature which, in turn, diminishes the induced flow due to thermal buoyancy effects. These behaviors are clearly seen from Figures 7 and 8. Also, it should be noted that for the case of heat generation ($\phi > 0$) the maximum fluid temperature does not occur at the wall but rather in the fluid layer adjacent to the wall as shown in Figure 8.

Figures 9 and 10 depict the influence of the Lewis number Le on the velocity and concentration profiles at $\xi = 1$ respectively. Increases in the values of the Lewis number result in decreasing the concentration distribution within the boundary layer. This decrease in concentration produces decreases in the

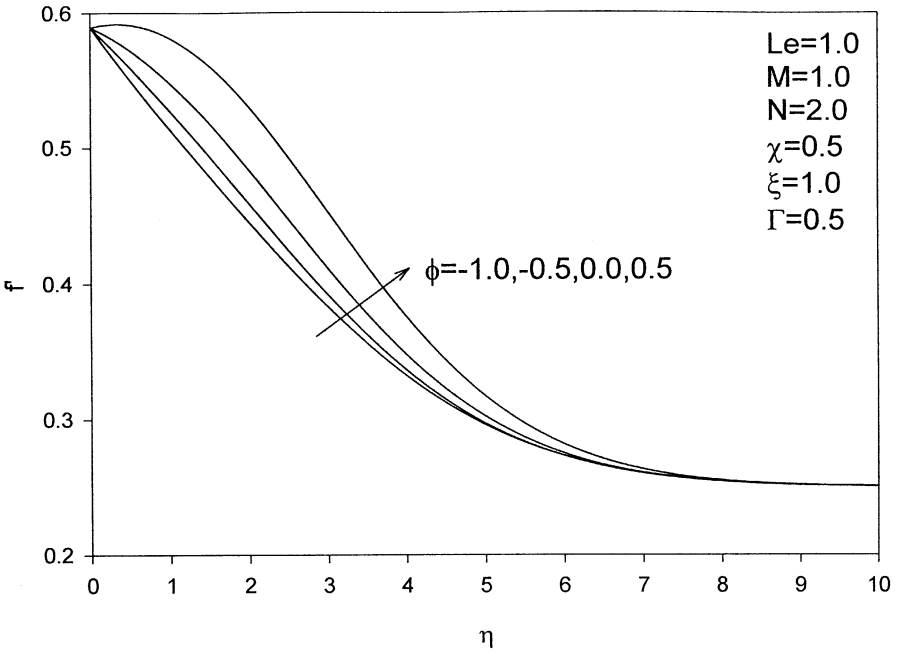

Figure 7.
Effects of ϕ on velocity profiles

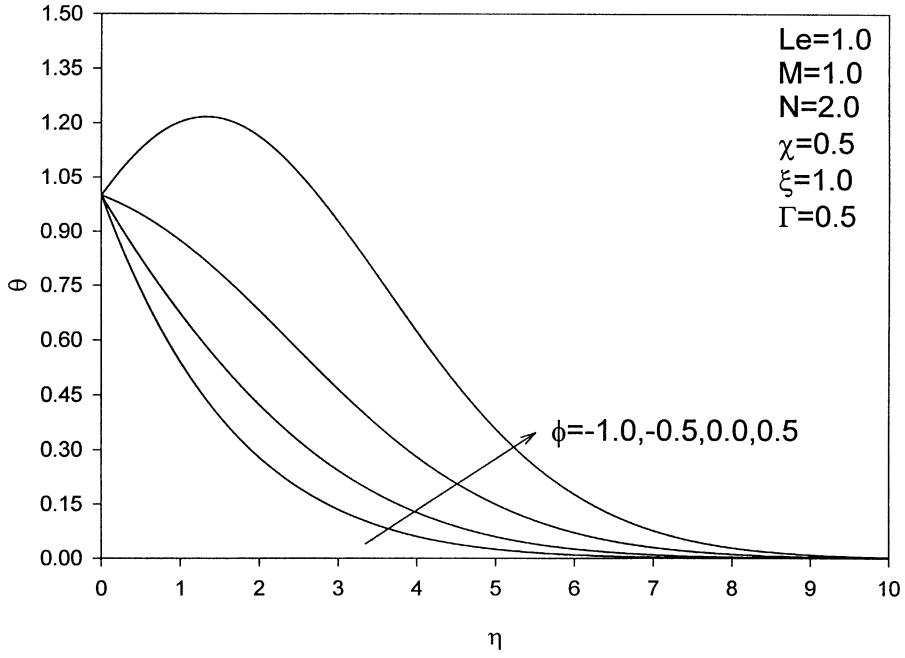

Figure 8.
Effects of ϕ on temperature profiles

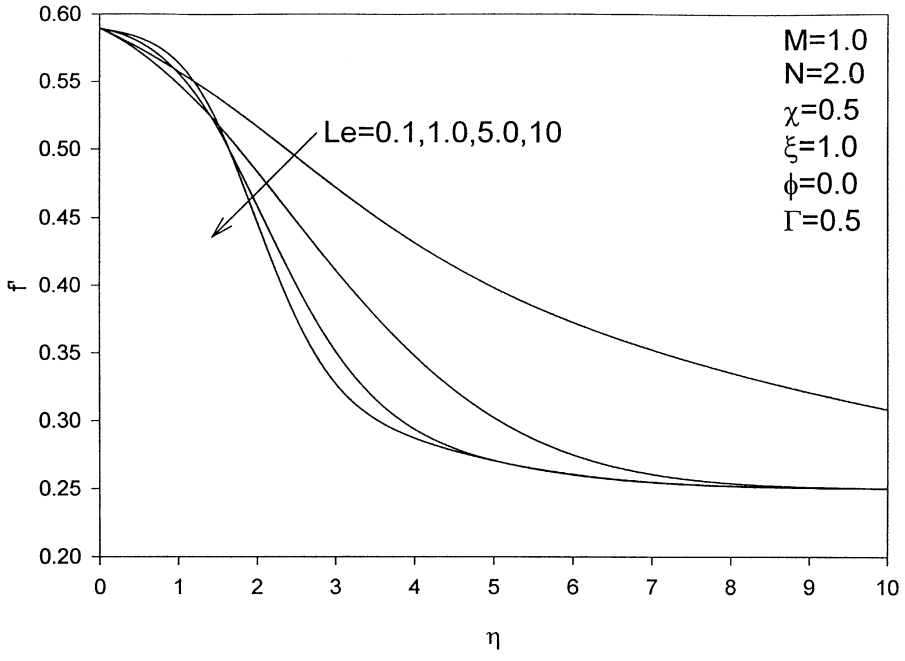

Figure 9.
Effects of Le on velocity profiles

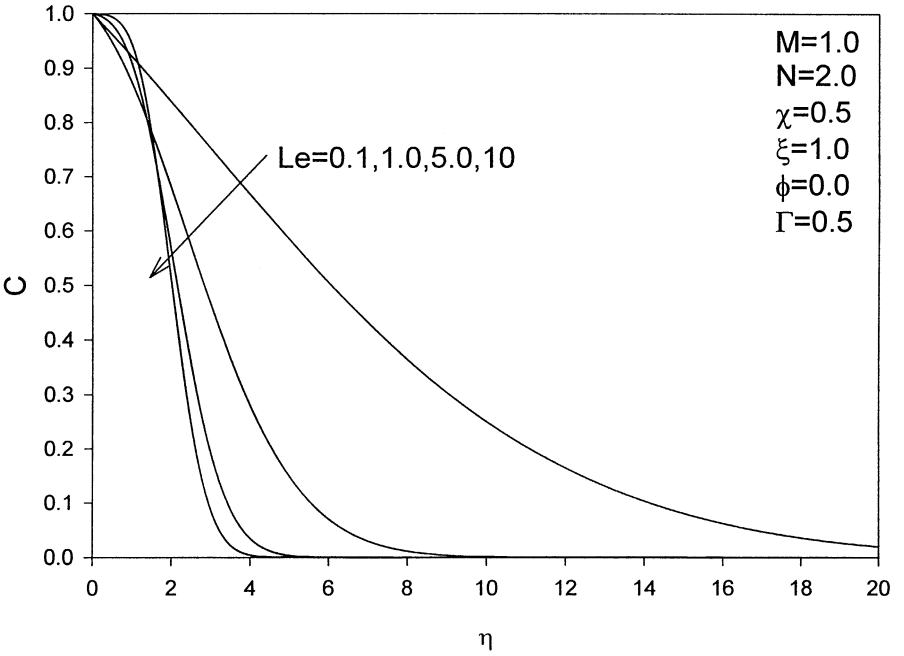

Figure 10.
Effects of Le on concentration profiles

induced flow due to the resulting reductions in the concentration buoyancy effects. It is seen from Figures 9 and 10 that increasing the value of Le causes both the velocity and concentration boundary layer thickness to decrease.

The porous medium inertia effects represented by Γ on the velocity and temperature (or concentration profiles) at $\xi = 1$ are shown in Figures 11 and 12 respectively. Obviously, the porous medium inertia parameter Γ provides a resistance to flow mechanism which causes the fluid to move at a slower rate and with an increased temperature and concentration. These behaviors are displayed in Figures 11 and 12.

Figure 13 illustrates the influence of the magnetic field on the Nusselt or Sherwood numbers Nu $(\mathrm{Nu}_x/(\mathrm{Pe}_x^{1/2} + \mathrm{Ra}_x^{1/2}))$ or Sh $(\mathrm{Sh}_x(\mathrm{Pe}_x^{1/2} + \mathrm{Ra}_x^{1/2}))$ at $\xi = 1$ in the entire regime of mixed convection $0 \leq \chi \leq 1$. For a specific value of χ other than $\chi = 1$, as the square of the Hartmann number M increases, the wall slopes of the temperature and concentration profiles increase as shown earlier in Figure 2 causing both the Nusselt and Sherwood numbers to decrease. This effect on Nu and Sh is more pronounced for relatively smaller values of M than for larger values as this effect becomes small. It is interesting to note that for smaller values of M ($0 \leq M \leq 1$) distinctive dips in the values of Nu and Sh occur in the range of $0 \leq \chi \leq 1$ and that these dips move in the direction of smaller χ values as M increases.

In Figure 14, the effects of the heat generation or absorption coefficient ϕ on the Nusselt number Nu at $\xi = 1$ in the entire mixed convection regime are shown. As seen earlier from Figure 8, the wall slope of the temperature profile

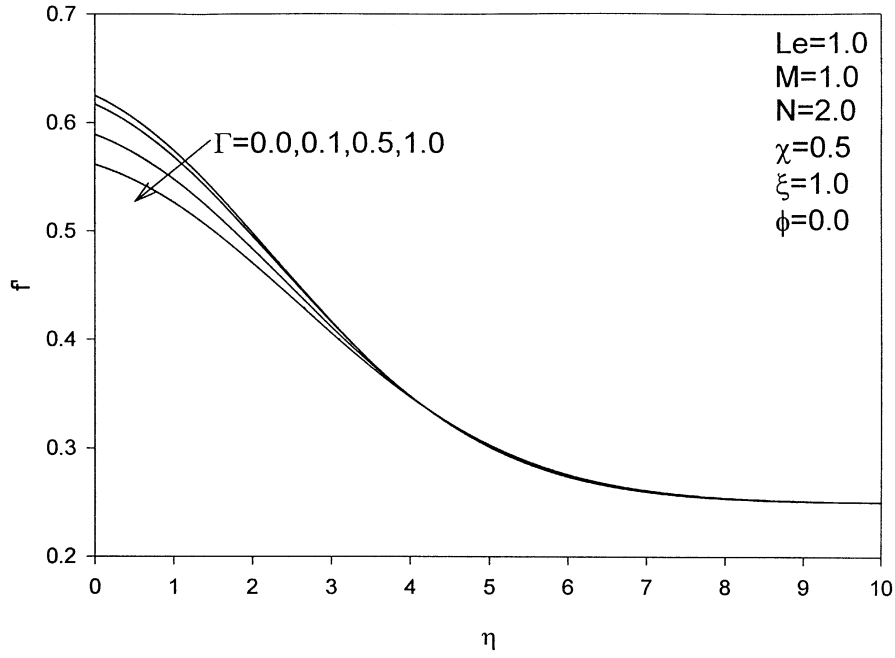

Figure 11.
Effects of Γ on velocity profiles

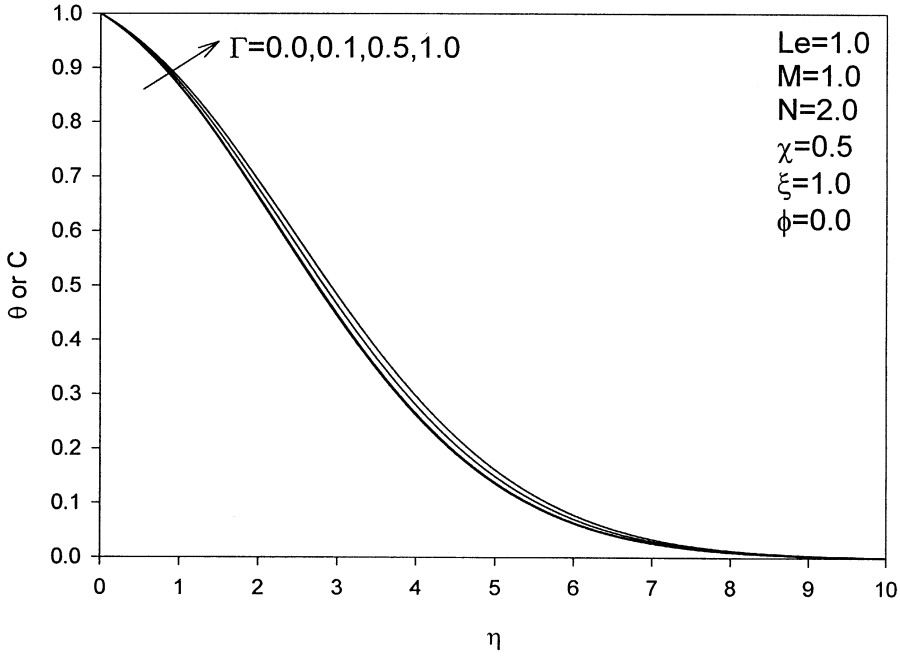

Figure 12.
Effects of Γ on temperature or concentration profiles

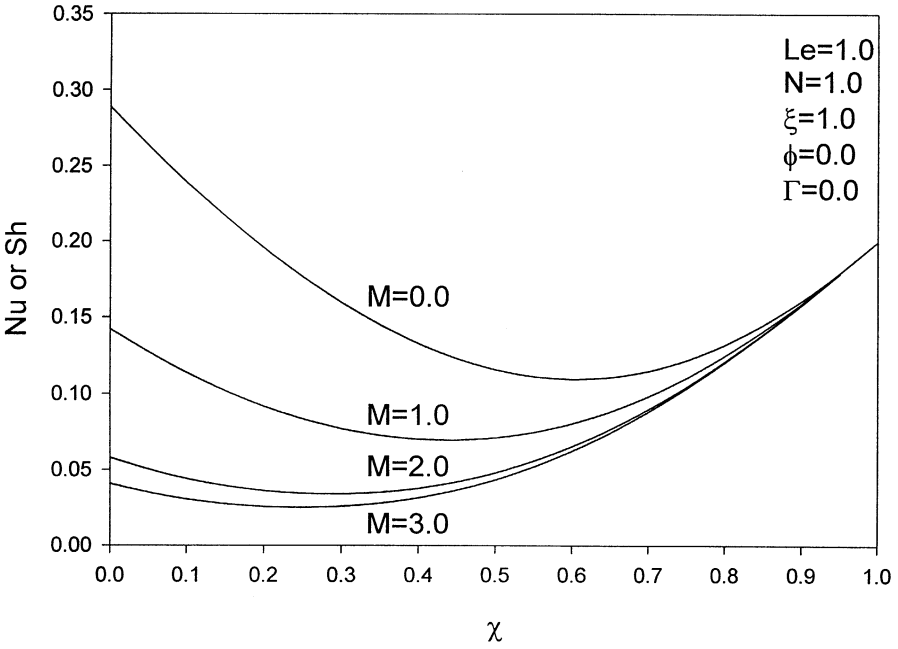

Figure 13.
Effects of M and χ on the Nusselt number

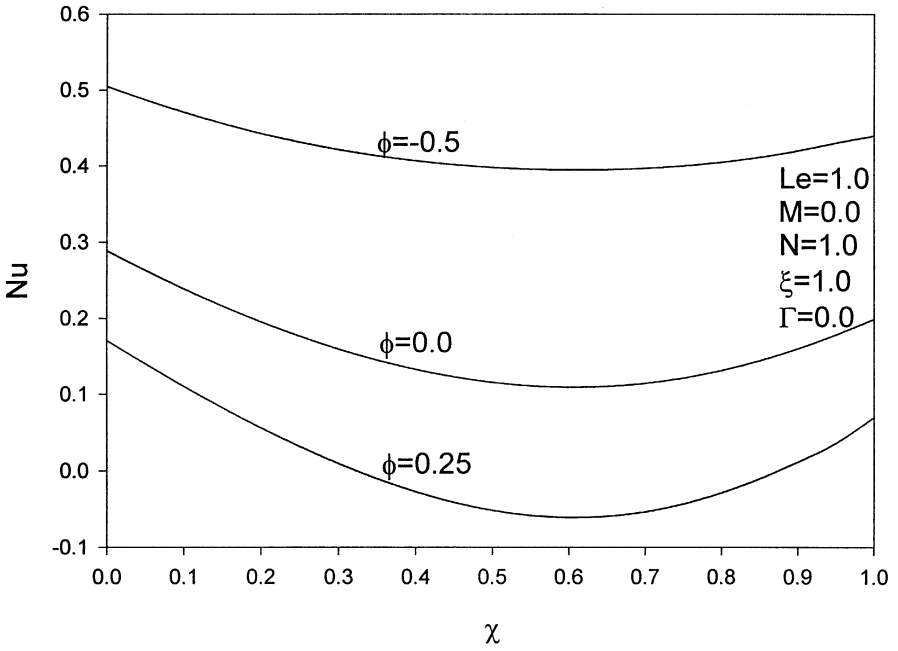

Figure 14.
Effects of ϕ and χ on the Nusselt number

increases as ϕ increases. This causes the Nusselt number which is directly proportional to $-\theta'(\xi, 0)$ to decrease as is obvious from Figure 14. For the heat generation case ($\phi = 0.25$) shown, the negative values in Nu for some values of

χ are due to the existence of fluid temperature peaks in the fluid layers adjacent to the wall for which the slope of the temperature profile at the wall $\theta'(\xi, 0)$ is positive, as discussed earlier.

Figure 15 displays the effects of the Lewis number Le on the Sherwood number Sh at $\xi = 1$ in the whole mixed convection range. It is predicted that the Sherwood number increases for increases of Le in the range of $0.1 \leq \mathrm{Le} \leq 1.0$ and decreases as Le is increased beyond Le = 1. Inspection of Figure 10 shows that the wall slope of the concentration profile at $\xi = 1$ decreases for $0.1 \leq \mathrm{Le} \leq 1.0$ while it increases for values of $\mathrm{Le} \geq 1$. These behaviors are consistent with the behavior of the Sherwood number for various values of Le as it is related to the negative wall slope of the concentration profile.

Finally, in Figure 16, the effects of the buoyancy ratio N and the transformed suction or injection parameter ξ on the Nusselt number Nu are displayed. It is noted that an increase in wall suction ($\xi < 0$) produces an increase in the local Nusselt number while an increase in injection ($\xi > 0$) results in lower surface heat transfer. This is consistent with the results reported earlier by Hooper *et al.* (1993). Obviously, increasing the buoyancy ratio N increases the flow along the plate and its temperature causing the negative wall slope of the temperature profile to increase. This yields enhancements in the wall heat transfer. These behaviors are evident from Figure 16.

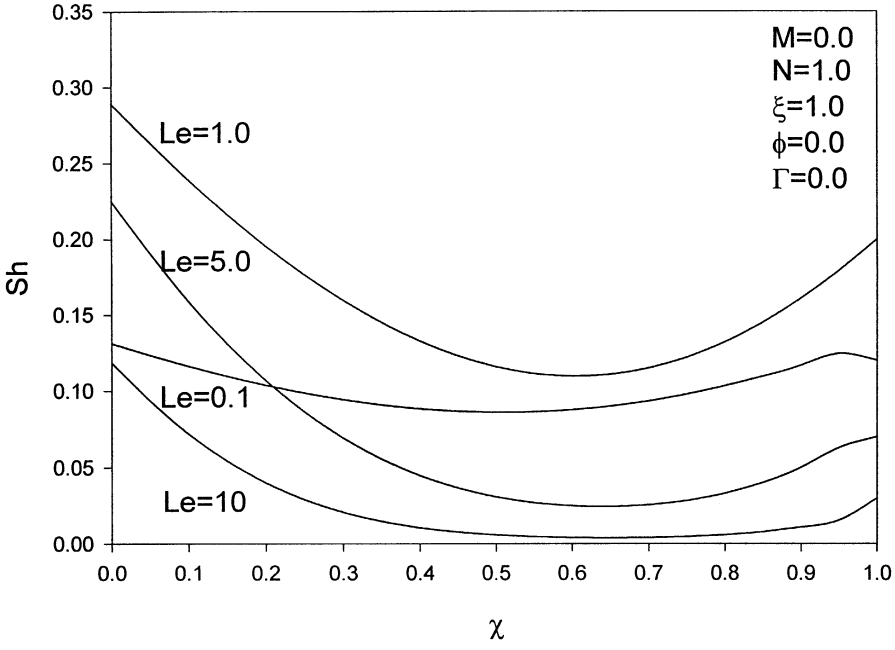

Figure 15.
Effects of Le and χ on the Sherwood number

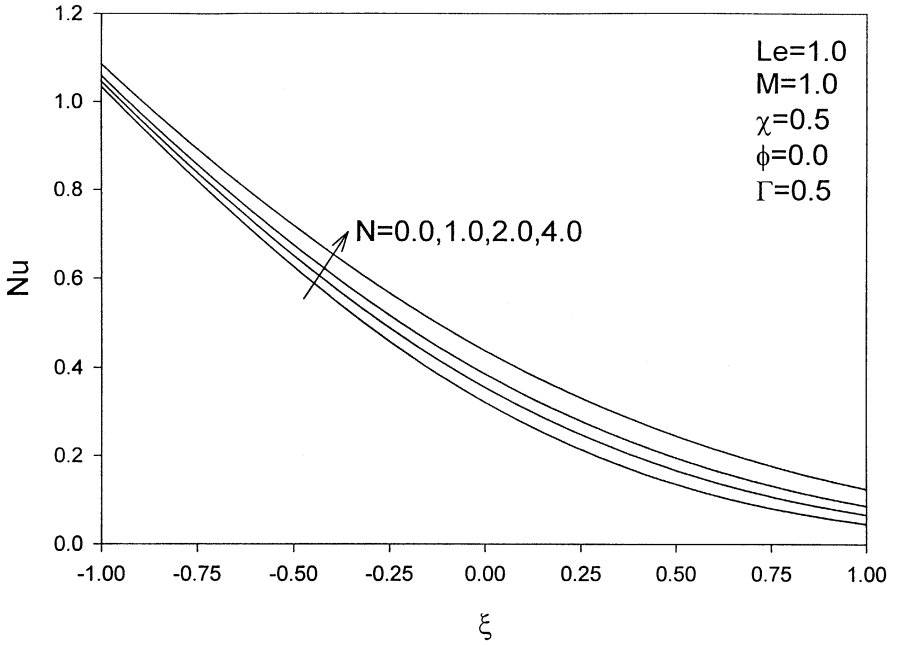

Figure 16.
Effects of N and ξ on the Nusselt number

Useful correlations

In this section, various correlations for the local Nusselt number Nu (and in one case the local Sherwood number Sh) as a function of either the mixed convection parameter χ, the Hartmann number M or the heat generation or absorption coefficient ϕ are reported.

First, correlations for Nu and Sh as functions of χ are found (with M = N = Le = $\xi = 1.0$ and $\Gamma = \phi = 0$) as follows:

$$\mathrm{Nu} = 0.1429 - 0.3298\chi + 0.3581\chi^2 + 0.03134\chi^3 \qquad \text{(C1)}$$

$$\mathrm{Sh} = 0.2901 - 0.5512\chi + 0.3536\chi^2 + 0.1090\chi^3 \qquad \text{(C2)}$$

The above correlations provide results that agree fairly well with the numerically predicted values. They are recommended for the entire range of mixed-convection regime ($0 \leq \chi \leq 1$) with each having a maximum error of 0.4 percent.

Second, a correlation for Nu as a function of χ is also found (with M = 0, N = Le, $\xi = 1.0$, $\Gamma = 0$ and $\phi = 0.25$) as follows:

$$\mathrm{Nu} = 0.1728 - 0.6613\chi + 0.3040\chi^2 + 0.2559\chi^3 \qquad \text{(C3)}$$

The above correlation has a maximum error of 1.1 percent.

Third, a correlation for Nu in terms of both χ and M (with N = Le = $\xi = 1.0$ and $\Gamma = \phi = 0$) is found as follows:

$$\mathrm{Nu} = 0.1305 - 0.2216\chi - 0.02914\mathrm{M} + 0.3407\chi^2 + 0.003236\mathrm{M}^2 \qquad \text{(C4)}$$

Correlation (C4) is suitable for $1 \leq M \leq 4$ and $0.25 \leq \chi \leq 1$ and has a maximum error of 20 percent. It is also found that if the range of χ is extended to include the free-convection limit ($\chi = 0$), and the range of M included the case where the magnetic field is absent, the maximum error increases to about 30 percent. For this case a correlation is given as follows:

$$\mathrm{Nu} = 0.1923 - 0.3173\chi - 0.058\mathrm{M} + 0.3833\chi^2 + 0.0088\mathrm{M}^2 \qquad \text{(C5)}$$

Fourth, a correlation for Nu which combines the effects of both χ and ϕ with M = 0, N = Le = ξ = 1.0, and Γ = 0) is found as follows:

$$\mathrm{Nu} = 0.2707 - 0.4842\chi - 0.2542\phi + 0.4055\chi^2 - 0.5084\phi^2 \qquad \text{(C6)}$$

The above correlation is valid for the ranges of $0 \leq \chi \leq 1$ and $-0.5 < \phi < 0$ and has a maximum error of 11 percent. If the range of ϕ is extended up to ϕ = 0.25, the maximum error increases to 23 percent. This correlation is found as follows:

$$\mathrm{Nu} = 0.2875 - 0.5868\chi - 0.5564\phi + 0.4975\chi^2 - 0.09543\phi^2 \qquad (7)$$

It should be mentioned that correlations for Nu as a function of positive or negative values of ξ were reported by Hooper *et al.* (1993). Therefore, none are shown here.

Conclusion

In this study, the effects of a temperature-dependent heat source or sink and magnetic field on heat and mass transfer by mixed convection from a vertical permeable plate in porous media were considered. A single parameter for the entire range of free-forced-mixed convection regime was employed. The obtained non-similar differential equations were solved numerically by the finite-difference methodology. Useful correlations for the local Nusselt number were reported. It was found that both the Nusselt and Sherwood numbers decreased due to the presence of a magnetic field for the whole range of free and mixed convection regime while they remained constant for the forced-convection regime. However, they decreased and then increased, forming dips as the mixed-convection parameter was increased from the free-convection limit to the forced-convection limit. The effect of heat generation (source) was found to decrease the Nusselt number while the opposite was predicted for heat absorption (sink) conditions. The Sherwood number was increased with increases in the Lewis number up to a limit, after which it decreased with further increases in the Lewis number.

References

Acharya, S. and Goldstein, R.J. (1985), "Natural convection in an externally heated vertical or inclined box containing internal energy sources", *J. Heat Transfer*, Vol. 107, pp. 855-66.

Aldoss, T.K., Al-Nimr, M.A., Jarrah, M.A. and Al-Sha'er, B.J. (1995), "Magnetohydrodynamic mixed convection from a vertical plate embedded in a porous medium", *Numer. Heat Transfer*, Vol. 28A, pp. 635-45.

Bian, W., Vasseur, P. and Meng, F. (1996), "Effect of electromagnetic field on natural convection in an inclined porous medium", *Int. J. Heat Fluid Flow*, Vol. 17, pp. 36-44.

Blottner, F.G. (1970), "Finite-difference methods of solution of the boundary-layer equations", *AIAA Journal*, Vol. 8, pp. 193-205.

Chamkha, A.J. (1996), "Non-Darcy hydrodynamic free convection from a cone and a wedge in porous media", *Int. Commun. Heat Mass Transfer*, Vol. 23, pp. 875-87.

Chamkha, A.J. (1997), "Non-Darcy fully developed mixed convection in a porous medium channel with heat generation/absorption and hydromagnetic effects", *Numer. Heat Transfer*, Vol. 32, pp. 853-75.

Cheng, P. (1977), "The influence of lateral mass flux on free convection boundary layers in a saturated porous medium", *Int. J. Heat Mass Transfer*, Vol. 20, pp. 201-6.

Cheng, P. and Minkowycz, W.J. (1977), "Free convection about a vertical flat plate embedded in a porous medium with application to heat transfer from a dike", *J. of Geophys. Res*., Vol. 82, pp. 2040-4.

Cheng, P., Ali, C.L. and Verma, A.K. (1981), "An experimental study of non-Darcian effects in free convection in a saturated porous medium", *Lett. Heat Mass Transfer*, Vol. 8, pp. 261-5.

Garandet, J.P., Alboussiere, T. and Moreau, R. (1992), "Driven convection in a rectangular enclosure with a transverse magnetic field", *Int. J. Heat Mass Transfer*, Vol. 34, pp. 741-8.

Hooper, W.B., Chen, T.S. and Armaly, B.F., "Mixed convection from a vertical plate in porous media with surface injection or suction", *Numer. Heat Transfer*, Vol. 25, pp. 317-29.

Hsieh, J.C., Chen, T.S. and Armaly, B.F. (1993), "Non-similarity solutions for mixed convection from vertical surfaces in a porous medium", *Int. J. Heat Mass Transfer*, Vol. 36, pp. 1485-93.

Khanafer, K. and Chamkha, A.J. (1998), "Hydrodynamic natural convection from an inclined porous square enclosure with heat generation", *Numer. Heat Transfer*, Vol. 33, pp. 891-910.

Lai, F.C. (1991), "Coupled heat and mass transfer by mixed convection from a vertical plate in a saturated porous medium", *Int. Commun. Heat Mass Transfer*, Vol. 18, pp. 93-106.

Lai, F.C. and Kulacki, F.A. (1990a), "The influence of surface mass flux on mixed convection over horizontal plates in saturated porous media", *Int. J. Heat Mass Transfer*, Vol. 33, pp. 576-9.

Lai, F.C. and Kulacki, F.A. (1990b), "The influence of lateral mass flux on mixed convection over inclined surfaces in saturated porous media", *J. Heat Transfer*, Vol. 112, pp. 515-18.

Minkowycz, W.J., Cheng, P. and Chang, C.H. (1985a), "Mixed convection about a non-isothermal cylinder and sphere in a porous medium", *Numerical Heat Transfer*, Vol. 8, pp. 349-59.

Minkowycz, W.J., Cheng, P and Moalem, F. (1985b), "The effect of surface mass transfer on buoyancy-induced Darcian flow adjacent to a horizontal heated surface", *Int. Commun. Heat Mass Transfer*, Vol. 12, pp. 55-65.

Nakayama, A. and Koyama, H.A. (1987), "General similarity transformation for free, forced and mixed convection in Darcy and non-Darcy porous media", *J. Heat Transfer*, Vol. 109, pp. 1041-5.

Ranganathan, P. and Viskanta, R. (1984), "Mixed convection boundary layer flow along a vertical surface in a porous medium", *Numerical Heat Transfer*, Vol. 7, pp. 305-17.

Raptis, A., Massias, C. and Tzivanidis, G. (1982a), "Hydromagnetic free convection flow through a porous medium between two parallel plates", *Phys. Lett*., Vol. 90A, pp. 288-9.

Song, T.-H. (1996), "Stability of a fluid layer with uniform heat generation and convection boundary conditions", *Int. J. Heat Mass Transfer*, Vol. 39, pp. 2378-82.

Vafai, K. and Tien, C.L. (1981), "Boundary and inertia effects on flow and heat transfer in porous media", *Int. J. Heat Mass Transfer*, Vol. 24, pp. 195-203.

Vajravelu, K., and Nayfeh, J. (1992), "Hydromagnetic convection at a cone and a wedge", *Int. Commun. Heat Mass Transfer*, Vol. 19, pp. 701-10.